

Phonon Softening and Elastic Instabilities in the Cubic-to-Orthorhombic Structural Transition of CsH

A.M. Saitta,^{1*} D. Alfè,^{1*} S. de Gironcoli,^{1*} and S. Baroni^{1,2*}

¹*INFN – Istituto Nazionale per la Fisica della Materia and*

SISSA – Scuola Internazionale Superiore di Studi Avanzati, Via Beirut 2-4, I-34014 Trieste, Italy

²*CECAM – Centre Européen de Calcul Atomique et Moléculaire, ENSL, 46 Allée d’Italie, 69364 Lyon Cedex 07, France*
(December 2, 2024)

The cubic-to-orthorhombic structural transition occurring in CsH at a pressure of about 17 GPa is studied by *ab initio* calculations. The relative stability of the competing structures and the transition pressure are correctly predicted. We show that this pressure-induced first-order transition is intimately related to a displacive second-order transition which would occur upon application of a shear strain to the (110) planes. The resulting instability is rationalized in terms of the pressure-induced modifications of the electronic structure.

PACS numbers: 62.50.+p 61.66.-f 63.20.Dj 63.75.+z

In recent years the availability of the diamond anvil-cell technology [1] has renewed the interest in the high-pressure properties of alkali halides which are the simplest and prototypical among ionic solids. In the case of cesium halides, these studies have been carried out especially in the search of band-overlap metallization which occurs at pressures in the Mbar range. In the quest of metallization, unexpected phase transformations to tetragonal and orthorhombic structures have been observed experimentally [2,3,4,5,6] and studied theoretically [6,7,8,9].

Metal hydrides are considerably more covalent than the corresponding halides. In fact, transition-metal hydrides are considered to be covalent materials, whereas alkali hydrides are structurally rather similar to the corresponding halides. Understanding the behavior of these materials at high pressure would presumably allow to better characterize the bonding properties of hydrogen in extreme pressure conditions and thus provide valuable hints towards the long searched goal of hydrogen metallization.

Alkali hydrides at zero pressure crystallize in the rock-salt (cubic $B1$) structure, while most of them undergo a transition to the cubic $B2$ (CsCl-like) structure at an applied pressure of a few GPa [10,11,12]. Recently, a second transition from the $B2$ structure to a new orthorhombic phase has been observed to occur in CsH at an applied pressure of about 17 GPa [13]. The new phase has been assigned the CrB structure which belongs to the D_{2h}^{17} space group.

In order to assess the driving mechanisms of the transition we have undertaken a series of first-principles calculations of the electronic, structural, elastic, and vibrational properties of CsH as well as of their dependence upon pressure. To this end, we have employed density-functional-theory (DFT) within the local-density approximation (LDA) [14], and its gradient-corrected (GC) generalizations [15]. Our calculations have been performed using norm-conserving pseudopotentials [16]. In the case

TABLE I. Comparison between calculated and experimentally observed structural properties of CsH. a_0 (a.u.) is the equilibrium lattice parameter in the $B1$ phase, B_0 (GPa) the bulk modulus, P_1^* and P_2^* the transition pressures (GPa) to the $B1$ and CrB structures respectively, while ΔV_1 and ΔV_2 are the corresponding volume changes. V_2^*/V_0 is the ratio of the volume at the $B2 \rightarrow$ CrB transition to the equilibrium volume.

	a_0	B_0	P_1^*	ΔV_1	P_2^*	ΔV_2	V_2^*/V_0
LDA	11.62	11.3	-0.8	18.0%	11	4.5%	0.63
GC	12.25	10.3	1.5	12.5%	15	4.0%	0.54
Expt. ^a	12.07	8.0	0.8	8.4%	17	6.3%	0.53

^aRef. [13]

of Cs, $5s$ and $5p$ semi-core states have been treated as valence states. For LDA calculations we have used the same Cs potential as in Ref. [8], while Hydrogen is described by a norm-conserving pseudopotential constructed for the $1s$ wave-function, so as to smoothen it somewhat and make our calculations well converged with the 25 Ry kinetic-energy cutoff which we use. New potentials have been generated for GC calculations. The vibrational properties are determined using the density-functional perturbation theory (DFPT) described in Ref. [17].

In Table I we report our results for some structural properties of CsH in the three phases studied here: $B1$, $B2$, and CrB. The LDA fails to account for the stability of the rocksalt structure at zero pressure (negative $B1 \rightarrow B2$ transition pressure), while GC calculations predict the correct sequence of transitions. GC-DFT also considerably improves the agreement between calculated and observed equilibrium lattice parameters and bulk moduli. The inclusion of Cs semi-core states in the valence manifold implies that the pseudopotential transferability is optimal around the corresponding orbital energies, rather than at the energies of the valence states. As a consequence, this treatment of semi-core states—although essential to obtain sensible results [8]—might require the use of more than one reference state in order

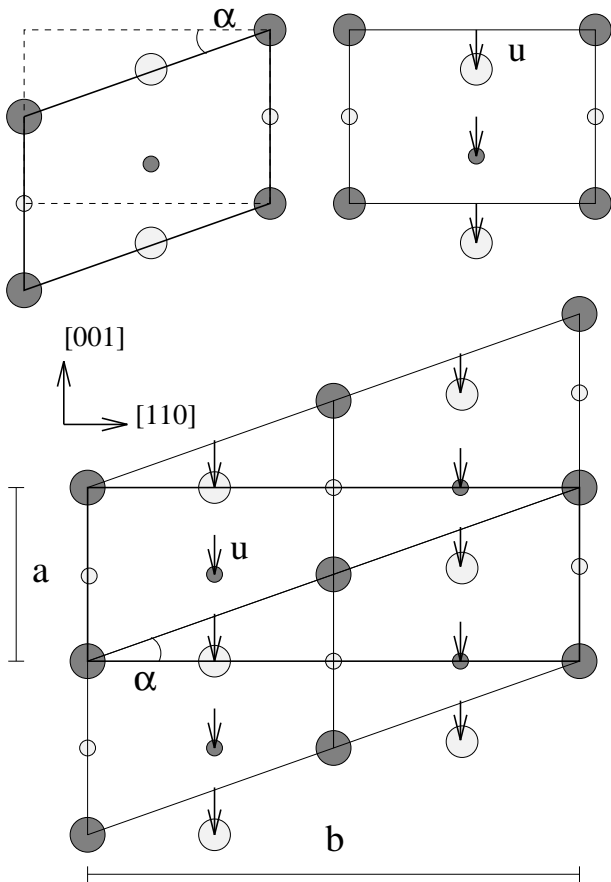


FIG. 1. Decomposition of the distortion leading to the CrB structure (lower panel) into an elastic (upper left) and a vibrational (upper right) contributions. Large and small circles represent Cs and H atoms respectively. Dark and light shading refer to the topmost and second (110) layers respectively

to ensure optimum transferability. Whether or not the relatively poor quality of the LDA predictions is due to deficiencies in the Cs pseudopotential and the improvements achieved by using GC-DFT due to a fortuitous cancellation of errors is a matter which deserves further investigations. In any events, our results seem to confirm the importance of the gradient corrections to the LDA in the description of structural phase transitions, recently claimed in the case of the diamond to β -tin transition in silicon [18]. Both LDA and GC-DFT calculations correctly predict that a transition from the $B2$ to the CrB phases would occur at pressures somewhat larger than 10 GPa. In this case too, GC-DFT gives a value of the transition pressure in closer agreement with experiments (15 *vs.* 17 GPa). Note however that—due to hysteresis effects—the experimental estimate done when loading the sample [13] only provides an upper limit to the transition pressure. Also the volume discontinuity and the ratio between the transition volume and the equilibrium one are well reproduced by our calculations.

The CrB structure can be viewed as resulting from a continuous deformation of the cubic $B2$ structure in

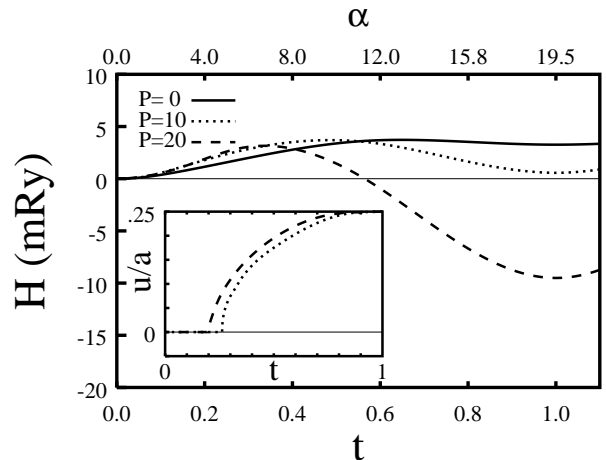


FIG. 2. Enthalpy *vs.* angle of deformation for different values of the applied external pressure. In the inset we show the corresponding values of the amplitude of the lattice distortion, u .

which a shear of the cubic edges in the (110) planes is coupled to a vibrational distortion of the atomic lattice, having the periodicity of a zone-border transverse phonon at the M point of the Brillouin zone (BZ), $\mathbf{q} = (\frac{1}{2}, \frac{1}{2}, 0)$, with symmetry M_2^- , and polarized along (001). In Fig. 1 we display how the distorted (110) plane (lower panel) results from the combination of the elastic (upper left) and the vibrational (upper right) deformations. In the ideal CrB structure the a and b crystallographic parameters indicated in Fig. 1 are in the ratio $b/a = 2\sqrt{2}$ which would be appropriate to a cubic structure. Due to the lower symmetry of the CrB structure with respect to the cubic one, the actual value of b/a slightly differs from the ideal one and depends somewhat on pressure. This dependence is however very weak: at the transition pressure, for instance, one has $b/a \approx 2.9$. The third crystallographic axis is orthogonal to the ab plane, and the corresponding crystallographic parameter has an ideal value $c = \sqrt{2}a$. The pressure dependence of c/a is somewhat stronger than that of b/a : at the transition, for instance, one has $c/a \approx 1.3$.

In Fig. 2 we show the $T = 0$ enthalpy, $H = E + PV$, of the system constrained to a given elastic deformation, as a function of its amplitude which we measure through the parameter $t = \tan(\alpha) \times b/a$ [19]. We see that at any positive pressure a second minimum exists for $t = 1$, corresponding to the CrB orthorhombic structure. Actually, the exact value of α slightly depends on pressure because so does b/a . For pressures higher than $P_2^* \approx 11$ GPa the second minimum becomes more stable giving rise to a first-order phase transition. The amplitude of the vibrational distortion, $u \equiv x/a$, which minimizes the enthalpy, u_{min} , depends on t , but for $t = 1$ it is constrained by symmetry to be $u_{min} = 1/4$, independent of pressure. The dependence of u_{min} upon the amplitude of the elastic distortion, t , is shown in the inset of Fig. 2. We see

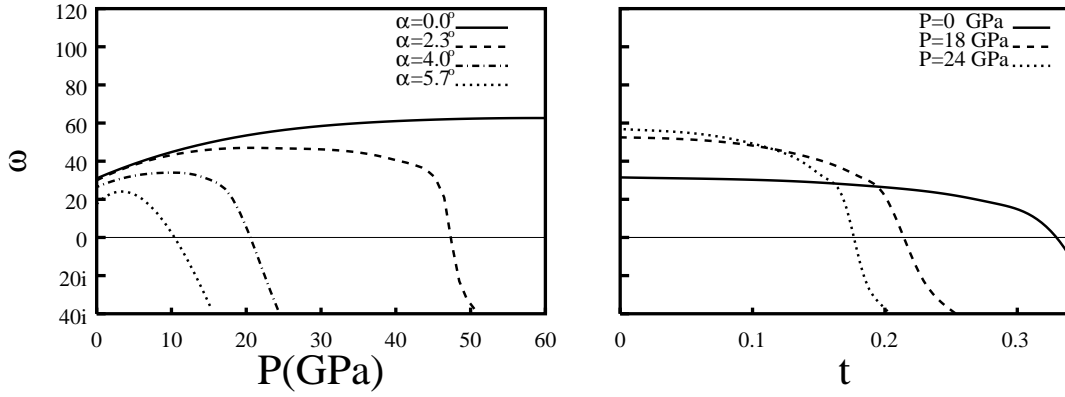


FIG. 3. Frequency of the M_2^- phonon mode (cm^{-1}) as a function of the applied hydrostatic pressure for different angles of deformation of the cubic structure (left), and as a function of the angle of deformation for different pressures (right).

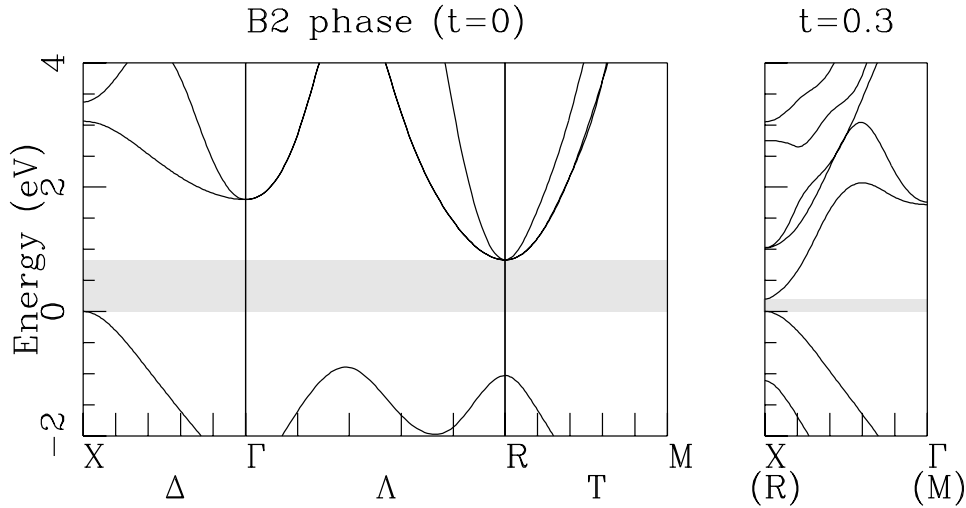


FIG. 4. Electron energy bands of CsH close the fundamental energy gap (which is evidenced by the shadowed area) at an applied pressure of 17.5 GPa in the cubic structure (left) and under a finite shear deformation (right)

that for $t^* < 1$ the $(1, \frac{1}{4})$ point is a minimum in the u direction, while nothing can be concluded in principle for other directions, but the fact that local stability is allowed. Our calculations indicate that in the present case $t^* < 1$ and that the CrB structure is indeed locally stable. For pressures higher than 11 GPa (15 GPa within GC), this structure is favored with respect to the cubic one, giving thus rise to a first-order transition.

The mechanisms driving the softening of the M_2^- phonon are related to the metallization of CsH under an applied pressure and/or shear deformation. At equilibrium ($P = 0$, $t = 0$), the maximum of the valence band is practically degenerate between the $R \equiv (\frac{1}{2}\frac{1}{2}\frac{1}{2})$ and $X \equiv (00\frac{1}{2})$ points of the BZ, and the minimum of the conduction bands lies at the R point. A small applied pressure lifts the degeneracy between the valence-band maxima, rising the X point with respect to R . The resulting fundamental band gap, E_g , corresponds therefore to a $X \rightarrow R$ transition, whose transferred momentum is

$M \equiv (\frac{1}{2}\frac{1}{2}0)$, *i.e.* the wave-vector of the phonon which goes soft.

In Fig. 4 we display the electronic energy bands of CsH at $P = 17.5$ GPa, for $t = 0$ and for $t = 0.3$. In the distorted structure—corresponding to a non-vanishing value of t —the R and X points are folded to a same point of the BZ, and so are the Γ and M points. The gap, which is indirect in cubic symmetry, becomes thus direct in the distorted structure. We see that the elastic distortion considerably favors metallization, and thus enhances the screening of the phonon frequencies at the M point of the cubic BZ. In Fig. 5 we display the dependence of E_g upon pressure and deformation angle. At small pressures, the M_2^- phonon frequencies softens almost for the same values of t for which the gap closes, whereas for pressure larger than ≈ 18 GPa, it takes a larger value of t to soften the phonon frequency than to close the

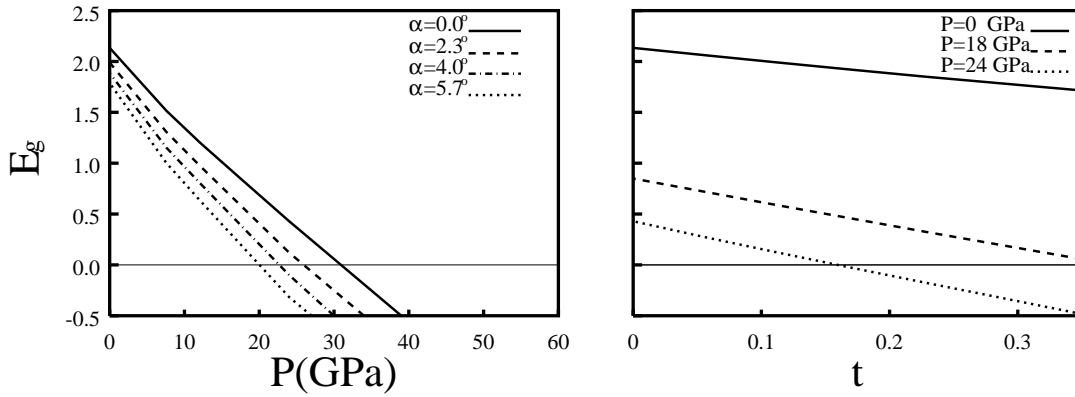


FIG. 5. Fundamental energy gap (eV) as a function of the applied hydrostatic pressure for different angles of deformation of the cubic structure (left), and as a function of the angle of deformation for different pressures (right).

gap. If the bands were parabolic around the valence- and conduction-band edges, the phonon would go soft at the metallization. In fact, the independent-electron polarizability, $\chi_0(\mathbf{q}_M)$ would diverge logarithmically in this case [20], and the restoring force for a lattice distortion of wave-vector \mathbf{q}_M would correspondingly vanish. If the valence and conduction bands have different shapes, the logarithmic divergence would no longer hold, and all that can be said in this case is that the more these shapes are similar, the more metallization contributes to the phonon softening. In any event, when the amplitude of the elastic distortion is larger than t^* , the spontaneous vibrational distortion due to phonon softening re-opens the band gap and makes the orthorhombic phase insulating, in agreement with the behavior of E_g found in [21].

We would like to thank J.-M. Besson and E. Tosatti for very useful discussions.

* Electronic addresses:

saitta@sissa.it, alfe@sissa.it, degironc@sissa.it, and baroni@sissa.it or baroni@cecam.it

- [1] H. K. Mao, *Simple molecular systems at very high density*, edited by A. Polian, P. Loubeyre and N. Boccara, NATO ASI Series, Series B: Physics **186**, 221, (1988).
- [2] E. Madelung, Phys. Z. **19**, 524 (1918); P. O. Ewald, Ann. Phys. (Leipzig) **64**, 253 (1921).
- [3] T. -L. Huang and A. Ruoff, Phys. Rev. B **29**, 1112 (1984); T. -L. Huang, K. E. Brister and A. L. Ruoff, Phys. Rev. B **30**, 2968 (1984); Y. K. Vohra, K. E. Brister, S. T. Weir, S. J. Duclos and A. L. Ruoff, Science **231**, 1136 (1986).
- [4] E. Knittle and R. Jeanloz, Science **223**, 53 (1984); E. Knittle and R. Jeanloz, J. Phys. Chem. Solids **46**, 1179 (1985); E. Knittle, A. Rudy and R. Jeanloz, Phys. Rev. B **31**, 588 (1985).
- [5] K. Asaumi, Phys. Rev. B **29**, 1118 (1984).
- [6] Y. K. Vohra, S. J. Duclos and A. L. Ruoff, Phys. Rev. Lett. **54**, 570 (1985).
- [7] N.E. Christensen and S. Satpathy, Phys. Rev. Lett. **55**, 600 (1985); S. Satpathy, N.E. Christensen, and O. Jepsen, Phys. Rev. B **32**, 6793 (1985).
- [8] S. Baroni and P. Giannozzi, Phys. Rev. B **35**, 765 (1987).
- [9] M. Buongiorno Nardelli, S. Baroni and P. Giannozzi, Phys. Rev. Lett. **69**, 1069 (1992); M. Buongiorno Nardelli, S. Baroni and P. Giannozzi, Phys. Rev. B **51**, 8060 (1995).
- [10] S. J. Duclos, Y. K. Vohra, A. L. Ruoff, S. Filipek and B. Baranowski, Phys. Rev. B **36**, 7664 (1987).
- [11] H. D. Hochheimer, K. Strossner, W. Honle, B. Baranowski, and S. Filipek, Z. Phys. Chem. **143**, 139 (1985).
- [12] I. O. Bashkin, V. F. Degtyareva, Y. M. Dergachev, and E. G. Ponyatovskii, Phys. Status Solidi (B) **114**, 731 (1982).
- [13] K. Ghandehari, H. Huo, A.L. Ruoff, S.S. Trail, and F.J. Di Salvo, Phys. Rev. Lett. **74**, 2264 (1995).
- [14] P. Hohenberg and W. Kohn, Phys. Rev. **136**, B864 (1964); W. Kohn and J.L. Sham, Phys. Rev. **140**, A1133 (1965).
- [15] In spite of the variety of available generalized gradient-corrections, we stick to a *standard* representative choice: exchange from A. D. Becke, Phys. Rev. A **38**, 3098 (1988) and correlation from J. P. Perdew, Phys. Rev. B **33**, 8822 (1986).
- [16] D.R. Hamann, M. Schlüter, and C. Chiang, Phys. Rev. Lett. **43**, 1494 (1979). L. Kleinman and D.M. Bylander, Phys. Rev. B **48** 1425 (1982).
- [17] S. Baroni, P. Giannozzi, and A. Testa, Phys. Rev. Lett. **58**, 1861 (1987); P. Giannozzi, S. de Gironcoli, P. Pavone, and S. Baroni, Phys. Rev. B **43**, 7231 (1990).
- [18] N. Moll, M. Bockstedte and M. Scheffler, Phys. Rev. B **52**, 2550 (1995).
- [19] The analysis which follows is based on calculations performed within the LDA. Our conclusions, of course, do not depend on the form of the exchange-correlation functionals.
- [20] The mathematical mechanism determining the logarithmic divergence of χ_0 is essentially the same as that responsible for the excitonic instability of semimetals, as explained *e.g.* in: W. Kohn, in *Many Body Physics*, Les Houches 1967, ed. C. DeWitt and R. Balian (Gordon and Breach, NY, 1968), p. 353.
- [21] K. Ghandehari, H. Huo, A.L. Ruoff, S.S. Trail, and F.J. Di Salvo, Solid State Commun. **95**, 385 (1995).